

# Hydroxyapatite coating on Ti6Al4V alloy by a sol–gel method

Diangang Wang · Chuanzhong Chen ·  
Ting He · Tingquan Lei

Received: 16 October 2006 / Accepted: 21 November 2007 / Published online: 12 December 2007  
© Springer Science+Business Media, LLC 2007

**Abstract** Using trimethyl phosphate and calcium nitrate tetrahydrate as the calcium and phosphorus precursors, respectively, HA films were prepared layer by layer by a sol–gel method. The phase constitution, microstructure and calcium/phosphorus (Ca/P) molar ratio of the sol–gel films were studied by X-ray diffraction (XRD) and electronic probe microanalysis (EPMA). The results show that the sol–gel films have high crystallinity and are composed of HA and CaO phases, and the Ca/P ratio is slightly higher than the theoretical value in HA because of the loss of phosphorous element. Two typical cauliflower-like and lamellar structures were observed in the films. Cauliflower-like structure, which increases the biological reactivity of the implant surface towards natural bone, formed mainly at low drying temperature and high calcining temperature, while the lamellar structure formed when the drying temperature is high (500 °C or above).

## 1 Introduction

Hydroxyapatite ( $\text{Ca}_{10}(\text{PO}_4)_6(\text{OH})_2$ , HA), which has the similar chemical composition and crystal structure to apatite in the human skeletal system, has raised much

interest as an implant material in clinic application [1]. Bone tissue can rapidly grow along the surface of the HA implant in the presence of a rich calcic and phosphorous environment, and firm chemical bonds can be formed between HA and bone tissues without any intervening soft tissue layer [2, 3]. Despite its excellent biocompatibility and efficacious biological fixation to bony tissues, the poor mechanical properties of HA in bulk form such as ductility and toughness restrict its use in load bearing applications [4]. HA is now often coated on a metal substrate such as titanium and its alloys as a new implant which combines the superior mechanical performance of the metal component with the excellent biological responses of the HA ceramic [5, 6].

In the past few years, various coating techniques have been used to produce HA layers, and the sol–gel technique has provided a number of advantages in preparing HA coatings [7–9]. One of the major advantages is the inherently low-temperature nature of the sol–gel process (including heat treatment for drying, calcining) which can restrain effectively the formation of amorphous phase. During the process of sol preparation, an atomic level of mixing ensures a significant improvement in the physical and chemical homogeneity of HA. Furthermore, the sol–gel process is easily applicable to substrates over a wide range of shape and size whereas it needs no high vacuum and no sophisticated equipments. The microstructure, phase constitution, biological performances and mechanical properties of the sol–gel HA films have widely studied [10–13]. It was found that crystalline HA can be obtained at calcined temperature ranging from 300 to 1,000 °C and the dominant phase in the films was HA with small amounts of calcium oxide, alpha tricalcium phosphate, beta tricalcium phosphate and so on [7, 14]. Hwang et al. reported that the sol–gel films prepared at

---

D. Wang · C. Chen (✉) · T. He · T. Lei  
School of Materials Science and Engineering,  
Shandong University, Jinan 250061, P.R. China  
e-mail: czchen@sdu.edu.cn

T. Lei  
School of Materials Science and Engineering, Harbin Institute  
of Technology, Harbin 150001, P.R. China

300 °C were very homogeneous and smooth, while the films exhibited small grains and pores at 500 °C and surface texture was obvious at 700 °C [15]. In Refs. [16, 17], the homogeneous, relatively rough and nano-porous structure was observed in the sol–gel films. The delaminated structure which weakens the bonding strength of the sol–gel films is also easily observed in the sol–gel films [10, 18], and during the thermal process, cracks were easily formed due to the shrinkage of the film [17, 19]. However the internal relations among technological parameters, structure and properties has not been studied systematically in the reported research. In this paper, bioactive HA films were prepared with trimethyl phosphate and calcium nitrate tetrahydrate by a sol–gel method, and the influence of drying and calcining temperature on the structures, the Ca/P molar ratio and the phase constitution of the sol–gel films was studied and internal relations among technological parameters, structure and properties was concluded.

## 2 Materials and methods

Commercial titanium alloy (Ti–6Al–4V, machined into  $10 \times 10 \times 12 \text{ mm}^3$ ) was selected as the substrate material and trimethyl phosphate (( $\text{CH}_3\text{O}$ )<sub>3</sub>PO, Kermel Chemical Industry, China) and calcium nitrate tetrahydrate ( $\text{Ca}(\text{NO}_3)_2 \cdot 4\text{H}_2\text{O}$ , Guangcheng Inc. China) were employed as the calcium and phosphate precursors.  $\text{Ca}(\text{NO}_3)_2 \cdot 4\text{H}_2\text{O}$  and ( $\text{CH}_3\text{O}$ )<sub>3</sub>PO were all dissolved in ethanol and a small amount of distilled water was added into the ( $\text{CH}_3\text{O}$ )<sub>3</sub>PO solution for hydrolysis. Once the two solutions clarified, they were mixed together to obtain sol with a same stoichiometric ratio of calcium to phosphorus as in HA, 1.67. After adding ammonia into the sol to adjust the pH value to be about 7.5, the sol was aged at 65 °C under stirring for about 12 h.

The HA films were prepared layer by layer as follows. Before coated with the sol, the substrates were polished and then cleaned in an ultrasonic bath of ethanol and/or acetone. After sol was coated on the substrates, a drying process was followed in a common furnace at 350 or 500 °C. Then the precoating and drying procedure was repeated 10 times. Finally, the dried layer was calcined at a higher temperature. The detail preparing procedures of each sample were shown in Table 1.

A JXA-8800R electron probe microanalyser (EPMA) with a Link ISIS300 energy spectrum analyser was used to give the structure image and determine element composition of the films and a D/max-rB X-ray diffractometer (XRD) was used to study the phase constitutions of the films.

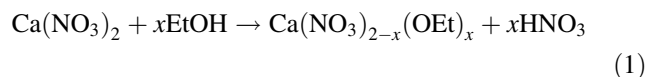
**Table 1** Processing parameters of preparing HA films on titanium alloy by sol–gel

No.	Drying temperature (°C)	Drying time (min)	Calcining temperature (°C)	Calcining time (min)
SG1	350	10	600	60
SG2	350	10	800	5
SG3	350	10	800	15
SG4	500	5	600	60
SG5	500	5	800	5
SG6	500	5	800	15

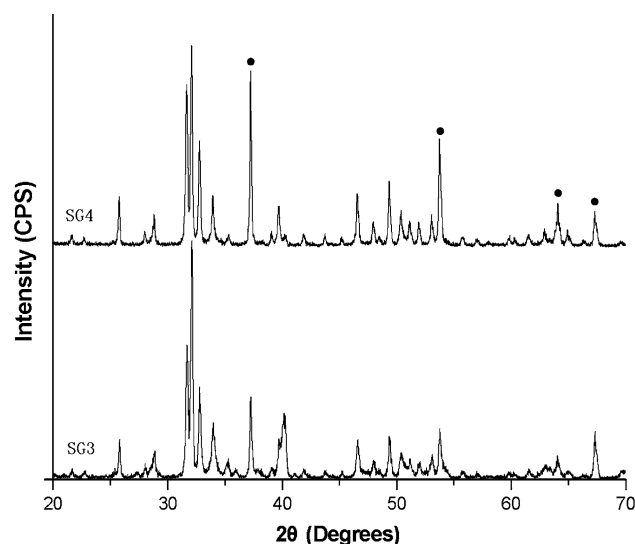
## 3 Results and discussions

Figure 1 is the X-ray diffraction patterns of the sample SG3 and SG4. It is clearly to see that the two samples have the similar X-ray diffraction patterns and are all composed of high crystalline HA and CaO phases. The results show that heat treatment temperature has little influence on the formation of HA phase, as is in accordance with some research results [7, 20] which stated that HA can be synthesized even at relatively low temperatures (300–400 °C) by a sol–gel method.

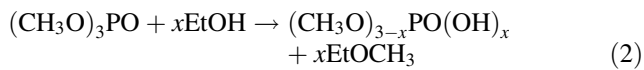
When  $\text{Ca}(\text{NO}_3)_2$  was dissolved into anhydrous ethanol, it may act with ethanol into  $\text{Ca}(\text{NO}_3)_{2-x}(\text{OEt})_x$  as follows [7]:



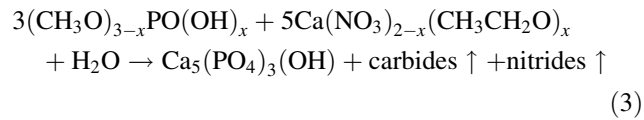
If water exists in the solution,  $\text{Ca}(\text{NO}_3)_2$  dissociates into  $\text{Ca}^{2+}$ . In ethanol solution, ( $\text{CH}_3\text{O}$ )<sub>3</sub>PO will hydrolyze into ( $\text{CH}_3\text{O}$ )<sub>3-x</sub>PO(OH)<sub>x</sub>, the reaction can be described by:



**Fig. 1** X-ray diffraction patterns of the sample SG3 and SG4 (•: CaO, others: HA)



During the sol was heat treated, HA is easily synthesized according to the following reaction:



On the other hand,  $(\text{CH}_3\text{O})_3\text{PO}$  can also change into volatilizable  $\text{P}_2\text{O}_5$ , consequently Ca/P ratio in the film increases and CaO phase forms which can be proved by the

X-ray diffraction spectra. CaO exhibits strong antibacterial activity in dental applications which is beneficial for the application of the films [21]. However because it is a strong base, CaO has serious cytotoxicity and can damage the living body by causing severe inflammation [22]. Therefore, the quantity of CaO should be reduced or be removed from the film by rinsing it in water since CaO readily dissolves. CaO is a bioinert phase which will weaken the bioactivity of the films and should try to reduce its formation. The content of CaO in sample SG4 is higher than that in SG3 is bewildering since the calcining temperature for SG4 is lower. Perhaps this is caused by its long treating time.

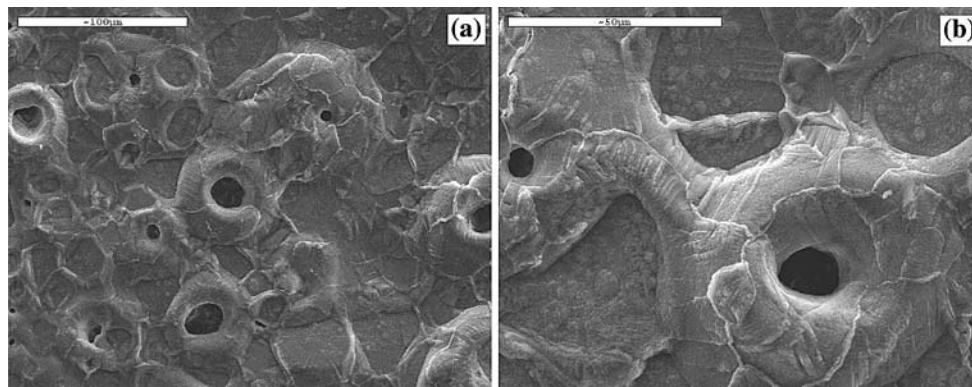


**Fig. 2** Surface morphologies of the sol-gel films dried at 350 °C and calcined at 600 °C (a) and (b) have different magnification

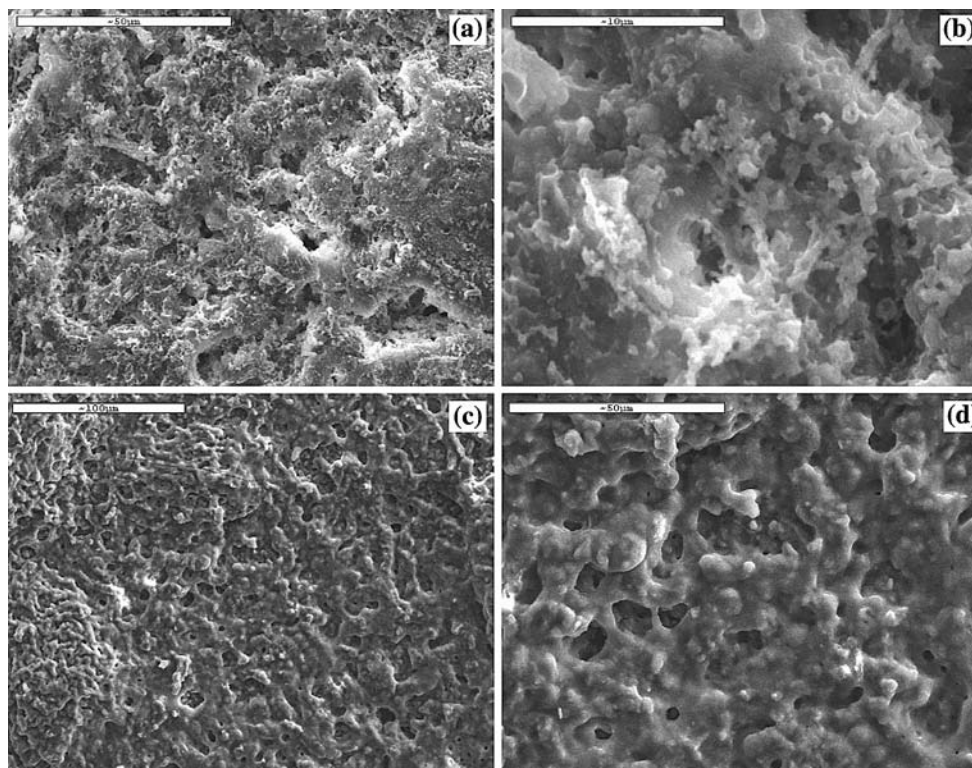


**Fig. 3** Surface morphologies of the sol-gel films dried at 350 °C and calcined at 800 °C (a) and (b): calcined for 5 min; (c) and (d): for 15 min

When the sol–gel film was dried at 350 °C and calcined at 600 °C, Fig. 2a shows that the film is not smooth and consists of some pores with the maximal dimension of about 20  $\mu\text{m}$ , and the grain boundary is obvious. There are clear surface texture in the film (see Fig. 2b) which will decrease the combination strength of the film. The composition analysis by energy dispersive X-ray spectroscopy (EDS) shows that the Ca/P ratio in the sol–gel film is 1.75 which is similar to the theoretical value 1.67 in HA.

Figure 3 shows the surface morphologies of the sol–gel films dried at 350 °C and calcined at 800 °C, it is clear to see that the surface texture disappears and the dimension of the pores decreases. The sol–gel film calcined for 5 min is composed of small grains and pores, and its surface is coarse and irregular which resembles the cauliflower-like geometry. This kind of structure has been observed in many references [23] and it can accumulate high surface energy, thus they have more activity. As an implant, its coarse surface can increase the mechanical interlocking of the films by the natural bone, resulting in stronger bonding between the bone and implant. When the film was calcined for 15 min, the surface is also coarse and even more homogeneous. The composition analysis by EDS shows that the Ca/P ratio in the sol–gel films calcined for 5 and 15 min is 1.82 and 1.96, respectively, which are all higher slightly than the theoretical value 1.67 in HA. When the film was treated at a high temperature, some volatilizable phosphide maybe formed and escaped from the film, so the Ca/P ratio increases and the redundant Ca element will form CaO as has been proved in the X-ray results.

From the back scattering electron (BSE) image of the cross-section of the sample SG2 and the EDS line analysis profiles (Fig. 4), it is shown that the film adhered well to the substrate and no obvious cracks were observed in the film. The distribution of Ca, P, O elements in the whole film is uniform except the content of P element in the bottom film is little higher because P is difficult to escape from the bottom film.

**Fig. 4** BSE images of the cross section of the sample SG2 (a) and EDS line analysis profiles (b)

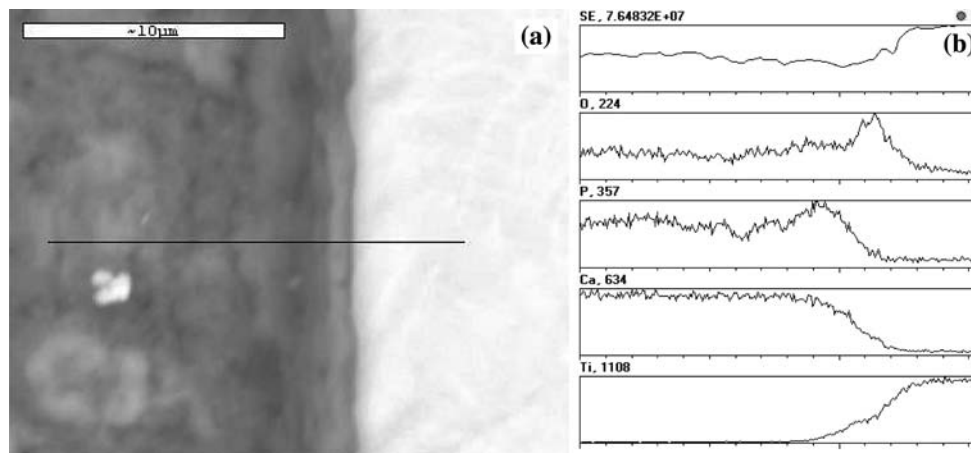
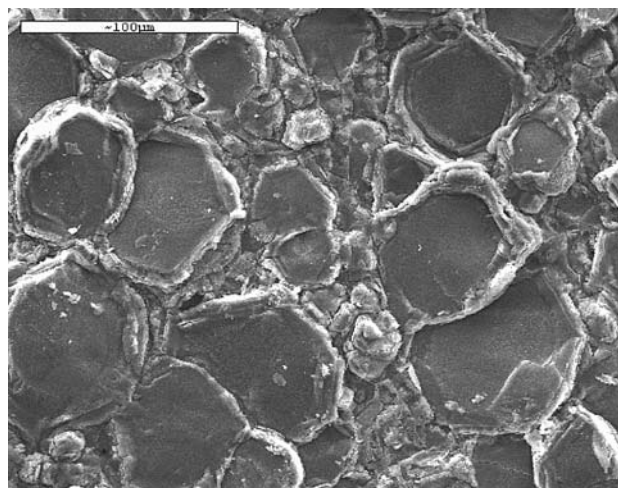
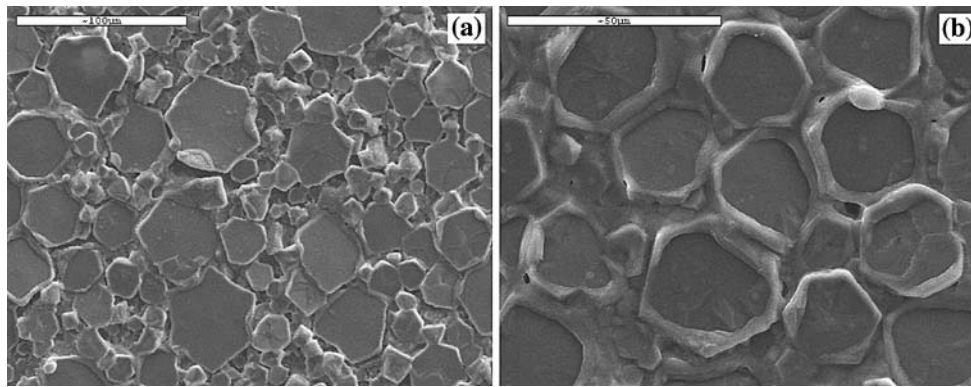


Figure 5 shows that the sol–gel films dried at 500 °C and calcined at 600 °C consists of lamellar structure while the whole surface is discontinuous and the lamellar structures don't connected well each other. The delamination phenomenon is severe and some fractal structure was observed which will weaken the bonding strength of the film. The Ca/P ratio of the film is 1.75 which is equal to that of sample SG1. When the film was calcined at 800 °C for 5 min, Fig. 6a shows that the lamellar structure is more regular and smooth, and the delamination phenomenon disappears, however the lamellar structure is still discontinuous. If delaying the calcining time to 15 min, Fig. 6b shows that the straight edges of lamellae changed into circular and the lamellae connected together.

From the above discussion, it can be clearly found that the drying temperature has the decisive role on the microstructure of the sol–gel film. In our experiments, we found that when the sol was dried at 350 °C, the dried layer was not steady and easily deliquesced in the atmosphere



**Fig. 5** Surface morphologies of the sol–gel films dried at 500 °C and calcined at 600 °C



**Fig. 6** Surface morphologies of the sol–gel films dried at 500 °C and calcined at 800 °C (a): calcined for 5 min and (b): for 15 min

after a certain time and would redissolve into the sol if the dried layer was immersed into the sol. According to a previous research [7, 24, 25], three weight loss stages of the coated sol can be easily distinguished during the heat treatment by a thermo-gravimetric analysis. The first weight loss (at 30–100 °C) indicates the evaporation of ethanol and distilled water, and the second weight loss (about at 200 °C) reveals the evaporation of crystalline water in  $\text{Ca}(\text{NO}_3)_2 \cdot 4\text{H}_2\text{O}$ , while the third weight loss (at 425 °C) implies the removal of  $\text{NO}_3^-$  groups. When the coated sol was drying at 350 °C, the ethanol, distilled and crystalline water will be removed from the sol while the  $\text{NO}_3^-$  groups still exist in the dried films, so the dried layer is easily redissolved into the sol. As the layer was repeatedly deposited for about 10 times to form the final film, the succedent deposited sol will redissolve the as-dried layer if the drying temperature is below 425 °C, so there was no interface between layers and no lamellar structure was observed in the final film. However when the drying temperature is 500 °C,  $\text{NO}_3^-$  groups have removed from the layer, so the final film consists of lamellar structure and delamination phenomenon is observed. For an implant, delamination can weaken its bonding strength [17], therefore, this kind of structure should be avoided by controlling the technological parameters.

#### 4 Conclusions

Using  $\text{Ca}(\text{NO}_3)_2$  and  $(\text{CH}_3\text{O})_3\text{PO}$  as the calcium and phosphorus precursors, respectively, HA films were easily synthesized by a sol–gel method. Besides HA phase, the bioinert CaO phase was also observed in the film. The technological parameters have little influence on the X-ray diffraction patterns of the films in this experiment, however with the increasing of the treating temperature and the delaying of the treating time, the Ca/P molar ratio increased because of the volatilization of phosphides.

Two typical structures were observed: cauliflower-like and lamellar structures, and the formation of the two different structures mainly depends on the drying temperature. When the drying temperature is low (for example 350 °C), the  $\text{NO}_3^-$  groups still exist in the dried layer, consequently, the as-dried layer will partly redissolve into the succedent sol deposited on it and no delamination generates. If the calcining temperature was low, the grain boundary was observed, and with the increasing the calcining temperature, cauliflower-like structure which conduces the bone tissue to embed deeply into the implants formed. When the drying temperature is high, the interface between layers is obvious and lamellar structure was observed. If the calcining temperature is 600 °C, delamination phenomenon is obvious, however the problem can be improved by increasing calcining temperature.

**Acknowledgements** This work is part of a research program financed by Promotional Fund of Scientific Research for Middleaged and Youthful Scientists of Shandong Province (Project No. 02BS056).

#### References

1. V. NELEA, C. MOROSANU, M. ILIESCU and I. N. MIHAILESCU, *Appl. Surf. Sci.* **228** (2004) 346
2. L.-G. YUA, K. A. KHORA, H. LIA and P. CHEANG, *Biomaterials* **24** (2003) 2695
3. K. A. KHOR and P. CHEANG, *J. Mater. Process. Technol.* **63** (1997) 271
4. Y. C. YANG and E. CHANG, *Biomaterials* **22** (2001) 1827
5. Q. BAO, C. CHEN, D. WANG, T. LEI and J. LIU, *Mater. Sci. Eng.* **A429** (2006) 25
6. Y.-P. LU, G.-Y. XIAO, S.-T. LI, R.-X. SUN and M.-S. LI, *Appl. Surf. Sci.* **252** (2006) 2412
7. D.-M. LIU, T. TROCZYNSKIA and W. J. TSENG, *Biomaterials* **23** (2002) 1227
8. A. BALAMURUGAN, G. BALOSSIER, S. KANNAN and S. RAJESWARI, *Mater. Lett.* **60** (2006) 2288
9. W. XU, W. Y. HU, M. H. LI, Q. Q. MA, P. D. HODGSON and C. E. WEN, *Trans. Nonfer. Metals Soc. China* **16** (2006) 209

10. S. ZHANG, Z. XIANTING, W. YONGSHENG, C. KUIA and W. WENJIAN, *Surf. Coat. Technol.* **200** (2006) 6350
11. J. HARLE, H.-W. KIM, N. MORDAN, J. C. KNOWLES and V. SALIH, *Acta Biomater.* **2** (2005) 547
12. K. CHENG, S. ZHANG, W. WENG and X. ZENG, *Surf. Coat. Technol.* **198** (2005) 242
13. W. XU, W. HU, M. LI and C. WEN, *Mater. Lett.* **60** (2006) 1575
14. C. M. LOPATIN, V. PIZZICONI, T. L. ALFORD and T. LAURSEN, *Thin Solid Films* **326** (1998) 227
15. K. HWANG and Y. LIM, *Surf. Coat. Technol.* **115** (1999) 172
16. H.-W. KIM, Y.-H. KOH, L.-H. LI, S. LEE and H.-E. KIM, *Biomaterials* **25** (2004) 2533
17. E. MILELLA, F. COSENTINO, A. LICCIULLI and C. MASSARO, *Biomaterials* **22** (2001) 1425
18. E. TKALCEC, M. SAUER, R. NONNINGER and H. SCHMIDT, *J. Mater. Sci.* **36** (2001) 5253
19. K. CHENG, S. ZHANG and W. WENG, *Thin Solid Films* **515** (2006) 135
20. J. ANDERSSON, S. AREVA, B. SPLIETHOFF and M. LINDÉN, *Biomaterials* **26** (2005) 6827
21. J. SAWAI, *J. Microbiol. Meth.* **54** (2003) 177
22. K. OZEKI, T. YUHTA, Y. FUKUI and H. AOKI, *Surf. Coat. Technol.* **160** (2002) 54
23. A. STOCH, W. JASTRZĘBSKI, E. DŁUGOŃ, W. LEJDA, B. TRYBALSKA, G. J. STOCH and A. ADAMCZYK, *J. Mol. Struct.* **744–747** (2005) 633
24. I.-S. KIM and P. N. KUMTA, *Mat. Sci. Eng.* **B111** (2004) 232
25. M.-F. HSIEH, L.-H. PERNG, T.-S. CHIN and H.-G. PERNG, *Biomaterials* **22** (2001) 2601